ASSESSING $PM_{2.5}$, AEROSOL, AND AEROSOL OPTICAL DEPTH CONCENTRATIONS IN HEFEI USING MODIS, CALIPSO, AND GROUND-BASED LIDAR

Zh. Fang [1,2,3], H. Yang [1,2,3], M. Zhao [1,3], Y. Cao [1,2,3], Ch. Li [1,2,3*], K. Xing [1,3], X. Deng [1,2,3], Ch. Xie [1,2,3], D. Liu [1,3]

[1] Key Laboratory of Atmospheric Optics, Anhui Institute of Optics and Fine Mechanics at Chinese Academy of Sciences, Hefei 230031, China; e-mail: fangzhy@mail.ustc.edu.cn
[2] Science Island Branch of Graduate School at University of Science and Technology of China, Hefei 230026, China; e-mail: yh9599@mail.ustc.edu.cn, caoye@mail.ustc.edu.cn
[3] Advanced Laser Technology Laboratory of Anhui Province, Hefei, 230037, China; e-mail: licheng5@mail.ustc.edu.cn, kunmingx@mail.ustc.edu.cn, dengxu@mail.ustc.edu.cn, zhaom@aiofm.ac.cn, cbxie@aiofm.ac.cn, dliu@aiofm.cas.cn

Due to the complications in the measurement of fine particulate matter ($PM_{2.5}$), this paper proposes a method using lidar for assessing $PM_{2.5}$. By calculating the aerosol optical depth (AOD) for MODIS, CALIPSO, and ground-based lidar, the corrected $PM_{2.5}$ was predicted. The results showed that AOD and $PM_{2.5}$ had a linear relationship. The linear correlation coefficient between ground-based lidar AOD and $PM_{2.5}$ was 0.81, and the root mean square error (RMSE) and mean deviation (MD) were 24.43 and 18.41, respectively. The linear correlation coefficient between CALIPSO AOD and $PM_{2.5}$ was 0.8, and its RMSE and MD were 42.91 and 33.25, respectively. The linear correlation between AOD and $PM_{2.5}$ for VIIRS was approximately 0.7. This paper provides more possibilities for lidar observation and prediction of the environment.

Keywords: *particulate matter $PM_{2.5}$, aerosol optical depth, aerosols, MODIS, CALIPSO, lidar.*

ОЦЕНКА КОНЦЕНТРАЦИИ МЕЛКИХ ТВЕРДЫХ ЧАСТИЦ В АТМОСФЕРЕ С ИСПОЛЬЗОВАНИЕМ ПРИБОРОВ MODIS, CALIPSO И НАЗЕМНЫХ ЛИДАРОВ

Zh. Fang [1,2,3], H. Yang [1,2,3], M. Zhao [1,3], Y. Cao [1,2,3], Ch. Li [1,2,3*], K. Xing [1,3], X. Deng [1,2,3], Ch. Xie [1,2,3], D. Liu [1,3]

УДК 551.594.25

[1] Аньхойский институт оптики и точной механики Китайской академии наук, Хэфэй 230031, Китай; e-mail: fangzhy@mail.ustc.edu.cn
[2] Филиал аспирантуры Университета науки и техники Китая, Хэфэй 230026, Китай; e-mail: yh9599@mail.ustc.edu.cn, caoye@mail.ustc.edu.cn
[3] Лаборатория передовых лазерных технологий провинции Аньхой, Хэфэй, 230037, Китай; e-mail: licheng5@mail.ustc.edu.cn, kunmingx@mail.ustc.edu.cn, dengxu@mail.ustc.edu.cn, zhaom@aiofm.ac.cn, cbxie@aiofm.ac.cn, dliu@aiofm.cas.cn

(Поступила 7 августа 2020)

Предложен метод оценки концентрации мелких твердых частиц $PM_{2.5}$ с использованием лидаров, учитывающий сложности в их измерении. Путем расчета аэрозольной оптической глубины (AOD) для приборов MODIS, CALIPSO и наземного лидара предсказана скорректированная оценка $PM_{2.5}$. Показано, что зависимость между AOD и $PM_{2.5}$ линейная. При измерениях наземным лидаром коэффициент линейной корреляции между AOD и $PM_{2.5}$ $R = 0.81$, среднеквадратичная ошибка $RMSE = 24.43$ и среднее отклонение $MD = 18.41$, для CALIPSO – $R = 0.8$, $RMSE = 42.91$ и $MD = 33.25$, для прибора VIIRS $R \sim 0.7$. Результаты представляют возможности для лидарного наблюдения и прогнозирования окружающей среды.

Ключевые слова: *твердые частицы $PM_{2.5}$, оптическая глубина, аэрозоль, MODIS, CALIPSO, лидар.*

Introduction. Air pollution is recognized as a major health risk today. In developing countries such as China, greater economic activities have led to higher levels of pollution in recent years. Industrial factories and cars contribute to most of the air pollution in most cities in China [1–3]. More seriously, low and middle-income countries are home approximately 80% of the world's population and account for approximately 90% of the deaths and nonfatal illnesses each year from air pollution [4].

Aerosols are solid or liquid particles that are suspended in the air and can form smog under certain conditions, and they have a direct impact on the visibility of the air and lead to atmospheric pollutants. In addition, aerosols can affect global and regional climates by scattering and absorbing solar radiation and by altering the radiation properties of clouds [5, 6]. Particulate matter (PM) is a generic term used for the mixture of offensive, inhalable particles in the air. PM_{10} and $PM_{2.5}$ refer to solid and liquid particles less than 10 and 2.5 μm in aerodynamic diameter, respectively [7, 8]. In the air, the fine fraction of PM_{10} and $PM_{2.5}$ pose high risks to healthy people, which increased the risk of cardiopulmonary disease by 6–13% per 10 $\mu g/m^3$ [7]; hence, these particles are considered air pollution-related challenges for health regulatory agencies. The aerosol optical depth (AOD), defined as the integration of the extinction coefficient of the medium in the vertical direction, is described as the reduction effect of aerosols on light. AOD is one of the most important parameters in aerosol research, and it is an optical parameter that represents the magnitude of depletion of solar insolation due to the scattering and absorption processes caused by aerosols. The satellite AOD, defined as the measure of the extinction of the solar beam by aerosols at a wavelength of 550 nm [9], has already been found to correlate well with PM measurements [10, 11]. AOD can also be derived from the aerosol extinction coefficient measured by lidar.

The methods for measuring $PM_{2.5}$ include gravimetric methods, beta-ray absorption and micro-oscillation. Due to errors in measurement equipment and methods, there is no instrumentation that can accurately determine the atmospheric concentration of $PM_{2.5}$. The methods mentioned are only conditionally available for monitoring $PM_{2.5}$. In addition, the process of $PM_{2.5}$ detections is complicated. Therefore, lidar measurements can be used not only to measure the extinction coefficient but also indirectly to predict the $PM_{2.5}$ content. This article focuses on assessing $PM_{2.5}$ using satellite and ground-based lidar, which can be used in monitoring and forecasting environmental pollution.

Experimental method. *Study area.* Covering a wide area of 11445 km^2, Hefei extends from latitude 30°57′N to 32°32′N and from longitude 116°41′E to 117°58′E. Hefei is in the middle-eastern portion of Anhui Province, and the difference between the highest and lowest points is 20 m. The Hefei metropolitan area has a population of almost 81.8 million residents (http://www.hefei.gov.cn/) and is one of the most important cities in East China. Poor air quality is mainly due to man-made factors such as rapid demographic expansion, rapid transformation of agricultural lands, and a rapidly growing number of cars. Hefei experiences a typical northern subtropical humid monsoon climate, with an annual average temperature of 15.7°C and annual average precipitation ranging from 800 to 1200 mm.

Ground-level $PM_{2.5}$ measurements. The hourly $PM_{2.5}$ concentrations during the study period are acquired from 10 stations run by the state control station of the Department of Ecological Environment of Anhui Province. We obtain the data from the website http://sthjt.ah.gov.cn/index.html. All stations are classified as center, east, north, south, or west. These stations are also used to monitor pollutants affecting air quality, including PM_{10}, SO_2, NO, CO, O_3, and humidity; therefore, all the factors can be used to analyze the $PM_{2.5}$ concentrations. Because of the finer resolution, hourly and daily $PM_{2.5}$ values are combined with daily averages if there are at least 10 observations on that day.

MODIS AOD. MODIS is a key instrument onboard NASA's Terra and Aqua satellites launched on 18 December 1999 and 4 May 2002, respectively [12]. MODIS AOD products have been extensively used for the estimation of PM [13–15]. Terra's orbit around the Earth is so timed that it passes from north to south across the equator (descending node) in the morning, while Aqua passes south to north over the equator (ascending node) in the afternoon [16]. The MODIS satellites pass over the study region twice a day, and specifically, Terra passes over between 11:00 and 12:00 h local time (LT), while Aqua passes over between 22:00 and 23:00 h LT. The MODIS Terra and Aqua satellites view the entire Earth's surface every one to two days and have been acquiring data since March 2000 (Terra) and July 2002 (Aqua) in 36 spectral bands between 0.4 and 14.4 μm [16].

The Visible Infrared Imaging Radiometer Suite (VIIRS) aboard the Suomi National Polar-orbiting Partnership (Suomi-NPP) spacecraft was launched in October 2011 [17]. It was designed to have many similar features as its predecessors, and its aerosol algorithm was also based on the MODIS Dark-Target algorithm. VIIRS is a cross-track scanning radiometer with 22 spectral bands covering the visible spectrum from 0.412

to 12.05 μm. VIIRS aerosol retrieval is performed at the pixel level and produces aerosol products with a spatial resolution of 0.75 km [18]. The product of this process, known as IP, is then aggregated and designated as an Environmental Data Record (EDR) reported at a 6-km resolution at nadir [19]. In this work, we evaluated VIIRS AOD 550s at the IP level. AOD 550s are the most important aerosol parameters used by models and other community-wide applications.

CALIPSO AOD. CALIPSO was launched in April 2006 under a joint mission of NASA and the French space agency, Centre National Etudes Spatiales (CNES). It is equipped with a dual-wavelength (532 and 1064 nm) polarization lidar system referred to as Cloud and Aerosol LiDAR with Orthogonal Polarization (CALIOP) for providing the long-term database of global aerosol vertical profiles [20]. CALIPSO aerosol level 2 provides extinction coefficients at 532 and 1064 nm, with a 5-km horizontal resolution and 60-m vertical resolution during daytime and nighttime. Due to its narrow swath, there is no CALIPSO overpass directly above Hefei. In this study, we use the average extinction coefficient when CALIPSO came near Hefei. In the data sets, the flag Atmospheric Volume_Description = 3 is used to ensure that the measured extinction coefficient belongs to aerosols (not clouds). The CAD_score and Extinction_QC_Flag_532 are also used for aerosol retrieval. In the daytime, because of sunlight contamination, the signal-to-noise ratio is relatively low in the observation. The AOD measured by CALIPSO can supplement the experimental results in this paper.

AOD values are normalized to aerosol layer height (ALH), and ALH can be computed from the weighted average of all data points in an atmospheric column in CALIPSO [21]. It can be expressed as

$$\mathrm{ALH}_{\mathrm{CALIPSO}} = \sum_1 h(l)\sigma(l) \Big/ \sum_1 \sigma(l), \tag{1}$$

where $\sigma(l)$ is the CALIPSO aerosol extinction (532 nm) of the vertical layer l defined by its mid-altitude $h(l)$.

Ground-based lidar AOD. According to the basic lidar principle, the equation of the received echo signal can be expressed as follows [22]:

$$P_L(z,\lambda_L) = (K_L / z^2)\beta(z,\lambda_L)\exp\left\{-2\int_{z_0}^{z}\alpha(z,\lambda_L)dz'\right\}, \tag{2}$$

where $P_L(z,\lambda_L)$ represents the lidar's return power, z is the distance between the lidar and target, K_L is the lidar constant, and $\beta(z,\lambda_L)$ is the backscattering coefficient of the scatter at height z at the wavelength of λ_L, which consists of backscattering coefficients of air molecules and aerosols; $\alpha(z,\lambda_L)$ is the extinction of the scatter at height z at a wavelength of λ_L, which is composed of the extinction coefficients of air molecules and aerosols and can be expressed as follows [22]:

$$\alpha(z,\lambda_L) = \alpha_a(z,\lambda_L) + \alpha_m(z,\lambda_L), \tag{3}$$

where $\alpha_a(z,\lambda_L)$ and $\alpha_m(z,\lambda_L)$ are the extinction coefficients of aerosols and air molecules, respectively; the backscattering coefficients and extinction coefficients of air molecules can be calculated from sounding data or standard atmospheric models based on Rayleigh scattering theory. At present, there are two main methods to solve the Mie scattering lidar equation: the Klett method and the Fernald method. The Fernald method is the most widely used; S_1 is the lidar ratio, and it changes largely for aerosols with different chemical and physical properties, but we assume it is constant with a value of 50 periods [23]; S_2 is the extinction backscatter ratio of air molecules, which can be obtained from Rayleigh scattering theory and can be written as $S_2 = 8\pi/3$ [24]. The calibration altitude L can be chosen at approximately 10 km, and by substituting (2), (3), and (4) into (1), the extinction coefficient of atmospheric aerosols can be described by the Fernald method [24]:

$$\alpha_a(z) = -\frac{S_1}{S_2}\alpha_m(z) + \frac{X(z)\exp[2(S_1/S_2-1)\int_z^{z_c}\alpha_m(z')dz']}{\dfrac{X(z_c)}{\alpha_a(z_c)+(S_1/S_2)\alpha_m(z_c)} + 2\int_z^{z_c}X(z'')\exp[2(S_1/S_2-1)\int_z^{z_c}\alpha_m(z')dz']dz''},$$
$$X(z_c) = P_L(z,\lambda_L)z_c^2. \tag{4}$$

The atmospheric extinction coefficient is an important parameter in the study of the vertical distribution of aerosols, while the aerosol loading in the atmosphere can be characterized by the AOD [25]. The AOD is the integral of the extinction coefficient along the optical path between z_1 and z_2:

$$AOD = \int_{z_1}^{z_2}\alpha(z)dr. \tag{5}$$

The AODs in the layer are from 0 to 3 km. The ground-based lidar has an overlap factor, so the lidar signals are removed from 0 to 150 m to avoid the effect of overlap height.

AOD-PM equator. Many scholars have studied the relationship between AOD and $PM_{2.5}$ among different places. Linear regression (LR) or multiple linear regression (MLR) are widely used to establish the relationship between AOD and $PM_{2.5}$, and this is widely and effectively used in the $PM_{2.5}$ prediction method [26]. A number of studies point out that there is a strong relationship between relative humidity (RH) and $PM_{2.5}$ [27], and it can be written as follows:

$$PM \approx \frac{\tau_{\alpha,\text{lidar}}}{\left[f(RH)\sigma_{dw,\text{lidar}}^{\alpha_{st}}\right]_{\text{surface}} L_{mix}}, \tag{6}$$

where $\tau_{\alpha,\text{lidar}}$ is the AOD calculated by lidar; $f(RH)$ is the hygroscopic growth factor simply expressed as $(1 - RH/100)^{-1}$; $\sigma_{dw,\text{lidar}}^{\alpha_{st}}$ is the aerosol extinction calculated by LiDAR; and L_{mix} is the mixing layer height (km). The increase in RH causes the escalation of light extinction due to hygroscopic growth of PM or photochemical phenomena [28]. In this method, it is necessary to modify the equation before any further analysis [29]:

$$\text{Corrected } PM = PM * f(RH), \tag{7}$$

$$\text{Normalized AOD}\left(\text{km}^{-1}\right) = \frac{\text{AOD}}{L_{\text{mix}} * \sigma_{dw,\text{lidar}}^{\alpha_{st}}}. \tag{8}$$

The value of AOD normalized by L_{mix} can be calculated by the extinction coefficient (km^{-1}) measured at the surface [29]. In this case, we can assume L_{mix} as the planetary boundary layer (PBLH) [30].

Results and discussion. *A case study of assessing $PM_{2.5}$ concentrations in Hefei.* Due to the alternation of the Siberian cold high-pressure and low-level warm air flow, Hefei experienced a weather phenomenon from mild pollution (54 μg/m^3 < $PM_{2.5}$ < 110 μg/m^3) to severe pollution (110 μg/m^3 < $PM_{2.5}$ < 170 μg/m^3), and then experienced sunny weather (0 μg/m^3 < $PM_{2.5}$ < 54 μg/m^3). This case is representative of winter days in Hefei because it contains three weather conditions: light pollution, heavy pollution, and sunny days; therefore, it can be used to analyze the distribution of $PM_{2.5}$ and AOD under different weather conditions.

Figure 1 shows the hourly changes in $PM_{2.5}$ and air quality from January 24 to 27. $PM_{2.5}$ data and relative humidity data for each hour are acquired through the website https://www.wunderground.com/history/daily/cn/hefei/ZSOF/date. The data show that the 24th and 25th days have higher $PM_{2.5}$ concentrations than the other days, which means that the content of $PM_{2.5}$ is several times that on the other days. At some hours, the level of severe pollution is reached.

Mie lidar detection. Mie lidar is an effective way to detect aerosols. In this article, we choose Mie lidar to analyze aerosols and calculate AOD in Hefei. The Mie lidar was installed on the science island of Hefei (31.52°N, 117.17°E) and obtained a large amount of experimental data from January 24 to 27, 2019, through four days of measurements. The laser system detects every 15 min and sends 5000 pulses each time. The frequency of the pulses is 20 Hz, with a 7.5-m spatial resolution in our lidar system.

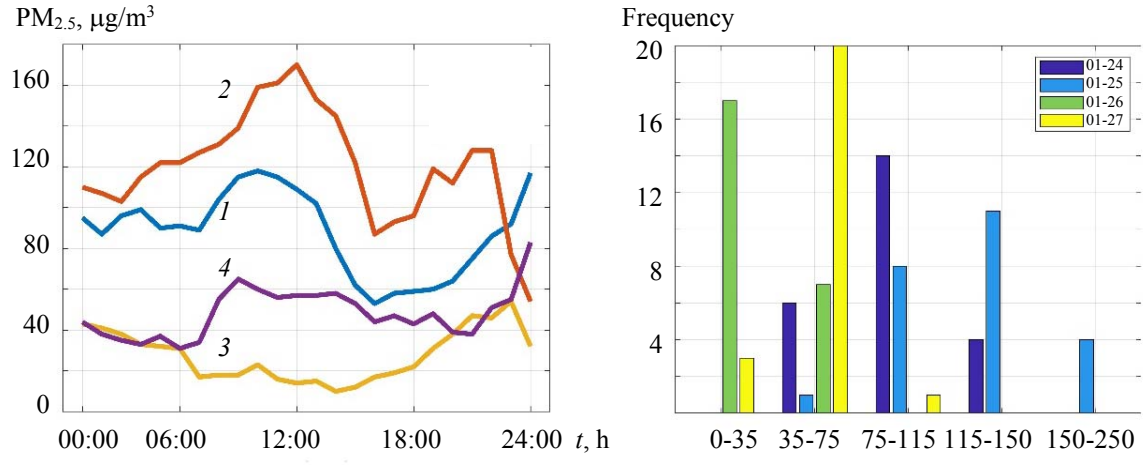

Fig. 1. Long-term diurnal patterns of $PM_{2.5}$ mass concentration and air quality standards: 01-24 (*1*), 01-25 (*2*), 01-26 (*3*), and 01-27 (*4*).

Figure 2 clearly shows the overall atmospheric changes in the altitude range of 0–5 km from January 24 to 27. The *X*-axis represents time, the *Y*-axis represents height, and the degree of the depth of color represents the backscattering intensity of the aerosols and clouds. Figure 2a shows that the clouds that have high reflectance is approximately 3 km in altitude and that there is a layer of aerosol on the ground. The range-corrected signal is calculated by Eq. (1). Clouds have a certain impact on the inversion results, and they block the diffusion of pollutants, which leads to slow air flow, increasing the concentration of pollutants in winter. In this article, the Fernald method is used to invert the extinction coefficient when there are no clouds, and it would change the lidar ratio and reduce the calibration point in cloudy weather to improve the accuracy of the extinction coefficient. The extinction coefficient at 532 nm is shown in Fig. 2b, and it can be seen that mostly at 12:00, the extinction coefficient is high, which means that there is severe pollution. Additionally, the coefficient is higher on January 24 and 25 than on January 26 and 27. In Figure 2c, the AOD is calculated by Eqs. (6) and (7). Given the effect of the overlap factor, since the overlap height of the lidar system is 150 m, the lidar signals from 0 to 150 m are removed. Most of the aerosols are below 2.5 km; therefore, the AOD is calculated from 150 m to 2.5 km in this article, and we eliminate the influence of clouds on the inversion by an algorithm. On January 25, the AOD has the highest level in the four days, and some of the values are over 1, which indicates severe weather conditions. However, the AOD on January 26 is at a low level, and the change in the extinction coefficient at 532 nm is smooth, which means that January 26 is a fine weather event.

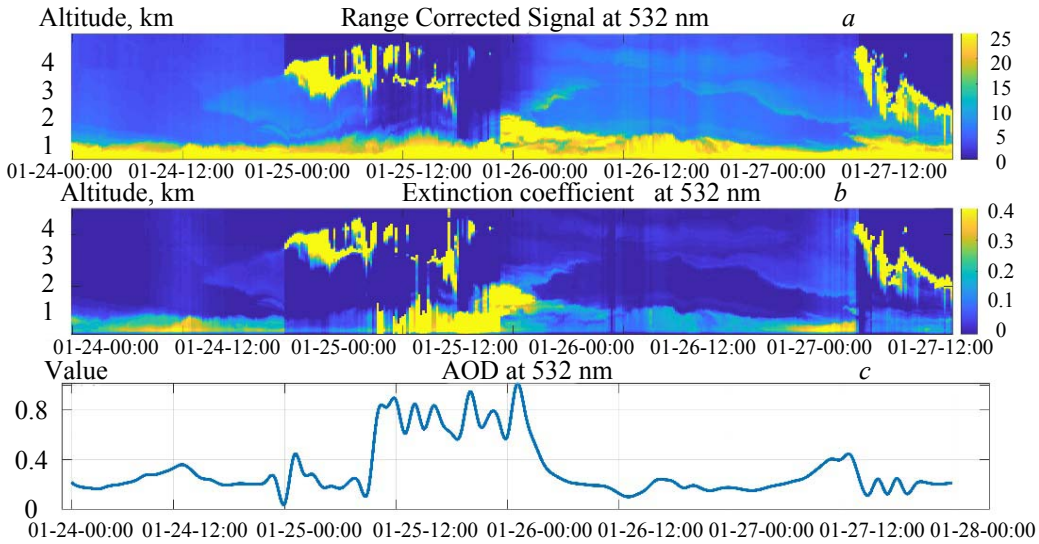

Fig. 2. Results of the ground-based lidar from January 24 to 27: (a) Range-corrected signal at 532 nm, (b) extinction coefficient at 532 nm, and (c) AOD at 532 nm.

Figure 3 shows the relationship between normalized $PM_{2.5}$ and ground-based lidar prediction from January 24 to 27. This article uses the west station $PM_{2.5}$ data and uses Eq. (9) to normalize the data. The AOD is calculated from Eq. (7), and then Eqs. (10) and (12) are used to obtain the ground-based lidar prediction. The prediction ability is evaluated using R-squared, RMSE, and MD as metrics. It is calculated between $PM_{2.5}$ and prediction vectors containing 96 data points. Hefei experienced weather with mild pollution to severe pollution to sunny weather, and then to more pollution on January 24 to 27, 2019; therefore, it is very representative to select these days. As seen, there is a strong correlation between the ground-based lidar prediction and normalized $PM_{2.5}$, and the correlation coefficient R is 0.81. The percentage of points near the expected-error (EE) line is relatively low, only 31%, the RMSE value is 24.43, and the mean deviation (MD) is 18.41.

MODIS detection. The AOD values of the four days during this weather process were selected, and the AOD values showed an obvious spatial gradient, which was larger in the north and smaller in the south of Hefei. The AOD values above the Hefei area were 0.79, 1.55, 0.39, and 0.85. During the occurrence of foggy-hazy weather, the increasing AOD value represents an increasing amount of aerosol-particle aggregation, which is basically consistent with the ground-based LIDAR observations.

As seen in Fig. 4, the fit curve between $PM_{2.5}$ and AOD can be obtained. This article uses AOD from the VIIRS Deep Blue Aerosol Optical Depth, which is the average of the daily AOD, and these values are used in combination with relevant data for correction. The data in VIIRS were selected for analysis because of the invalid samples in MODIS Terra and Aqua. This article selected 16 valid samples in VIIRS, and the range of satellite transit in the Hefei area is 200 km. The results show that the correlation coefficient is 0.7 between the original $PM_{2.5}$ and AOD, and the correlation coefficient is 0.68 with corrected $PM_{2.5}$. Therefore, the results show that there is a small effect on the corrected results.

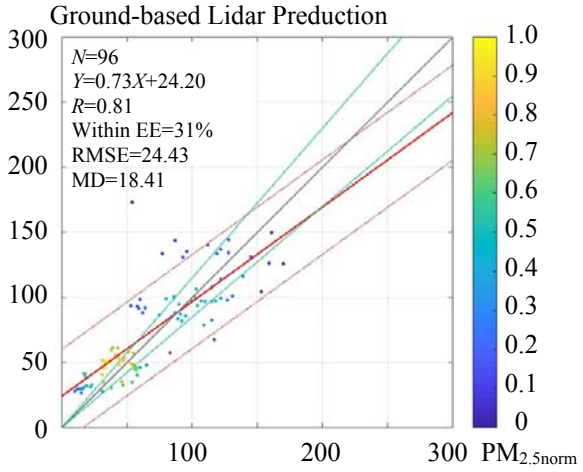

Fig. 3. Color scatterplots of the normalized $PM_{2.5}$ and ground-based lidar prediction from January 24 to 27. The color bar indicates the number of data points, the red-solid line is the linear regression, the gray-solid line is the 1:1 line, and the dashed-green lines are the expected-error (EE) envelopes. *N* is the number of statistics.

CALIPSO detection. CALIPSO has a 16-day revisit cycle; therefore, CALIPSO's ground track can cover the whole world every 16 days. Figure 5 shows a color image of the 532 nm backscatter coefficient of CALIPSO. Figure 5a shows the transit color chart on January 25 (UTC), and Fig. 5b shows the transit color chart on January 26. The color bar on the left side indicates the concentration of pollutants, and the red line indicates the position with latitude and longitude close to Hefei. It can be seen from Fig. 6 that the background light is relatively strong during the day, and therefore the signal is lower in the day. However, at night, as the influence of most background light decreases, the signal-to-noise ratio is relatively high, and therefore a high-quality signal can be obtained. From the figure, it can also be seen that cirrus clouds are mostly distributed at an altitude of 3 km, and clouds also exist at an altitude of 8 km.

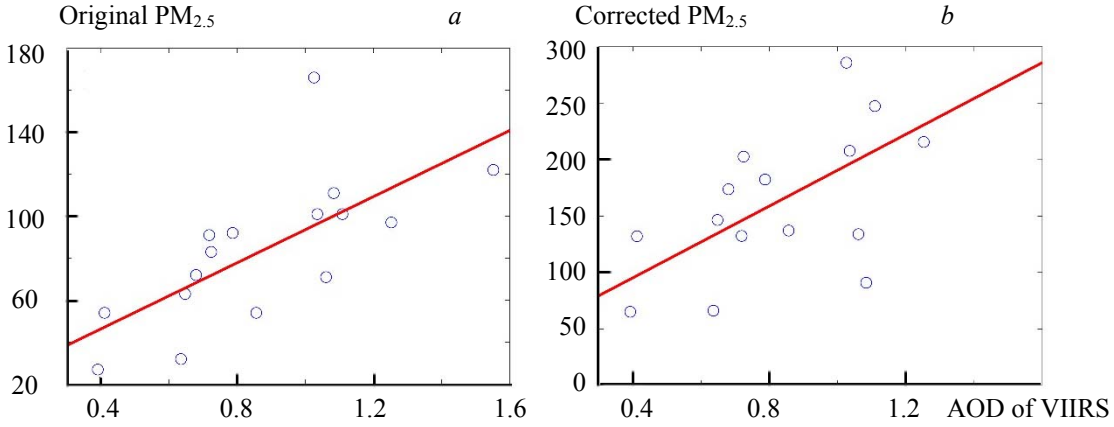

Fig. 4. The fit curve of MODIS AOD and $PM_{2.5}$: (a) AOD and original $PM_{2.5}$ fit curve; (b) AOD and corrected $PM_{2.5}$ fit curve; $R = 0.70$ (a), $R = 0.68$ (b).

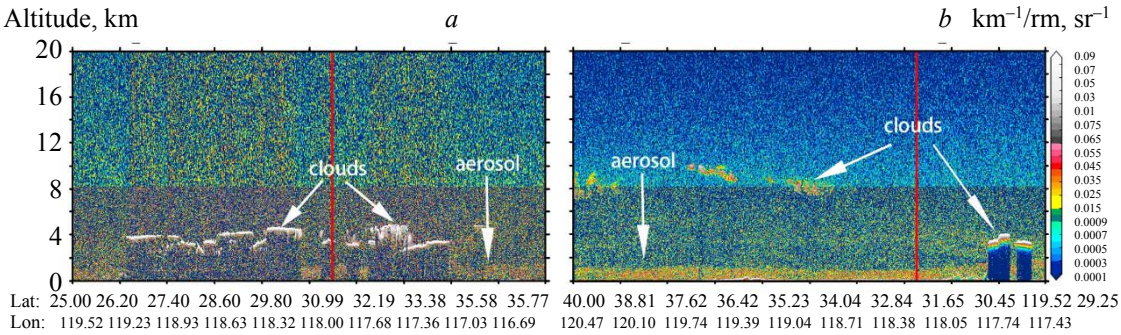

Fig. 5. Color chart of the CALIPSO backscatter coefficient.

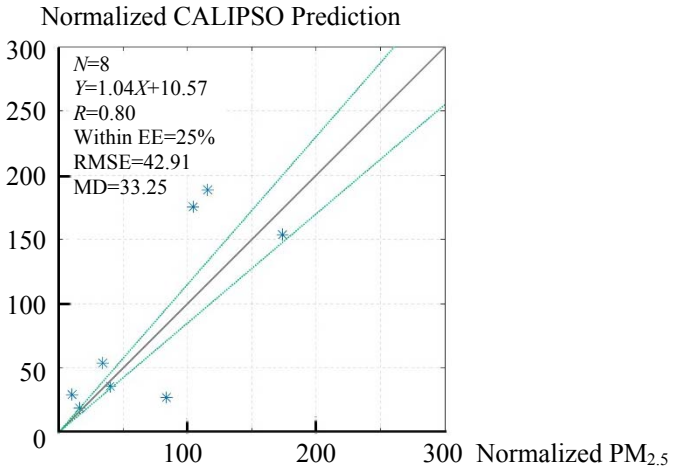

Fig. 6. The fit curve of the normalized $PM_{2.5}$ and normalized CALIPSO prediction.

Figure 6 shows the fitting diagram of the corrected $PM_{2.5}$ and CALIPSO predicted values. In this paper, we choose the data from January 2019 and the range of 120-km crossings by CALIPSO in the Hefei area as the effective radius and ignore the invalid value of the data. Then eight samples are extracted for prediction. According to Eqs. (2), (8), and (9), the boundary layer and analysis of the AOD are calculated. From the figure, it can be seen that the correlation coefficient R = 0.8, the RMSE = 42.91, and the MD = 33.25. Therefore, this method has a certain correlation, but the deviation is larger than that of the ground-based lidar.

Conclusions. $PM_{2.5}$ is evaluated by using the observed values of ground-based lidar and satellite lidar, and the following conclusions are obtained. The city of Hefei is located on a plain, and there is no special terrain, such as desert or ocean. The average altitude is 20–40 m, so the influence factors of terrain can be ignored in AOD. The research results show that the AOD of the day has been processed as the mean value in the VIIRS data. Lidar is an effective way to assess the atmospheric environment. Ground-based lidar is more accurate in predicting $PM_{2.5}$ concentrations. The combination of satellite-borne lidar and ground-based lidar can better predict $PM_{2.5}$. There are few samples used in this paper; ground-based lidar only uses four days in January, and satellite lidar uses effective samples in January. There are many factors influencing the prediction of the $PM_{2.5}$ value, many of which have nonlinear relationships. Large samples and data are needed for corresponding analysis in future research.

Acknowledgements. This work was supported by the Strategic Priority Research Program of Chinese Academy of Sciences (Grant No. XDA17040524) and Key Program of 13th five-year plan, CASHIPS (Grant No. KP-2019-05, D040103).

REFERENCES

1. C. K. Chan, X. Yao, *Environment*, **42**, 1–42 (2008).
2. D. W. Dockery, C. A. Pope III, X. Xu, J. D. Spengler, J. H. Ware, M. E. Fay, B. G. Ferris Jr., F. E. Speizer, *N. Engl. J. Med*., **329**, 1753–1759 (1993).
3. B. R. Gurjar, A. Jain, A. Sharma, A. Agarwal, P. Gupta, A. S. Nagpure, J. Lelieveld, *Atm. Environ.*, **44**, 4606–4613 (2010).
4. WHO, Ambient Air Pollution: A Global Assessment of Exposure and Burden of Disease (2016).
5. V. Ramanathan, P. J. Crutzen, J. T. Kiehl, et al., *Science*, **294**, No. 5549, 2119–2124 (2001).
6. Z. Pan, F. Mao, W. Gong, Q. Min, W. Wang, *Remote Sens. Environ.*, **198**, 363–368 (2017).
7. WHO, Health Effects of Particulate Matter. Policy Implications for Countries in Eastern Europe, Caucasus and Central Asia. World Health Organization (2013).
8. M. Vallius, *Characteristics and Sources of Fine Particulate Matter in Urban Air*, National Public Health Institute (2005).
9. Y. Choi, Y. Ghim, B. Holben, *Atm. Chem. Phys. Discuss.*, 26627–26656 (2013).
10. D. A. Chu, Y. Kaufman, G. Zibordi, J. Chern, J. Mao, C. Li, B. Holben, *Geophys. Res.: Atm*., **108** (2003).
11. P. Gupta, S. A. Christopher, J. Wang, R. Gehrig, Y. Lee, N. Kumar, *Atm. Environ.*, **40**, 5880–5892 (2006).
12. A. Savtchenko, D. Ouzounov, S. Ahmad, J. Acker, G. Leptoukh, J. Koziana, D. Nickless, *Terra and Aqua MODIS products available from NASA GES* (2004).
13. http://dx.doi.org/10.1016/j.asr.2004.03.012.
14. X. Yap, M. Hashim, *Atm. Chem. Phys. Discuss*., **12** (2012).
15. Y. Chu, Y. Liu, X. Li, Z. Liu, H. Lu, Y. Lu, Z. Mao, X. Chen, N. Li, M. Ren, *Atmosphere*, **7**, 129 (2016).
16. K. Ashish, S. Narendra, S. R. Anshumali, *Remote Sens. Environ.*, **206**, 139–155 (2018).
17. C. Cao, F. J. De Luccia, X. Xiong, R. Wolfe, F. Weng, *Remote Sens.*, **52**, 1142–1156 (2014).
18. H. Liu, L. A. Remer, J. Huang, H.-C. Huang, S. Kondragunta, I. Laszlo, M. Oo, J. M. Jackson, *Res. Atm*., **119**, 3942–3962 (2014).
19. D. M. Winker, M. A. Vaughan, A. Omar, Y. Hu, K. A. Powell, Z. Liu, W. H. Hunt, S. A. Young, *Atm. Measur.*, **26**, No. 11, 2310–2323 (2009).
20. D. M. Winker, et al., *Am. Meteorol. Soc.*, **91**, N 9, 1211–1229 (2010).
21. J. Chimot, J. P. Veefkind, T. Vlemmix, P. F. Levelt, *Atm. Measur. Tech.*, **11**, 2257–2277 (2018).
22. F. G. Fernald, *Opt. Appl.*, **23**, No. 5, 652 (1984).
23. J. Zhou, G. Yue, C. Jin, F. Qi, D. Liu, H. Hu, Z. Gong, G. Shi, T. Nakajima, T. Takamura, *Geophys. Res.*, **107**, D15, 4252–4259 (2002).
24. D. C. Wu, *Lidar Measurement of Atmospheric Aerosols and Water Vapor*, Hefei Institute of Physical Science, Chinese Academy of Sciences (2011).
25. B. M. Liu, Y. Y. Ma, Y. F. Shi, Y. B. Jin, W. Gong, *Atm. Res.*, **241**, 104959 (2020).
26. T.-C. Tsai, Y.-J. Jeng, D. A. Chu, J.-P. Chen, S.-C. Chang, *Atm. Environ.*, **45**, 4777–4788 (2011).
27. R. R. Draxler, G. D. Hess, *Aust. Metorol. Mag*., **47**, 295–308 (1998).
28. A. A. Chudnovsky, P. Koutrakis, I. Kloog, S. Melly, F. Nordio, A. Lyapustin, Y. Wang, J. Schwartz, *Atm. Environ.*, **89**, 189–198 (2014).
29. O. N. Seyed, H. Leopold, A. Esmail, *Atm. Pollut. Res.*, **10**, 889–903 (2019).
30. H. Liu, L. A. Remer, J. H.-C. Huang, S. Kondragunta, I. Laszlo, M. Oo, J. M. Jackson, *Geophys. Res. Atm*., **119**, 3942–3962 (2014).